Supporting Information

Synthesis of first mixed azido/phenoxido bridged trinuclear Cu(II) complexes of Mannich bases by metalloligand approach: Structures, magnetism and catalytic oxidase activities

Avijit Das[a], Kisholoy Bhattacharya[a,b], Lakshmi Kanta Das[c], Sanjib Giri[a,d], Ashutosh Ghosh*[a]

[a]*Department of Chemistry, University College of Science, University of Calcutta, 92, A. P. C. Road, Kolkata 700009, India, E-mail: ghosh_59@yahoo.com*

[b]*Department of Chemistry, Adamas University, Barasat-Barrackpore Road, Barasat 700126, West Bengal, India.*

[c]*Department of Chemistry, Government General Degree College at Kharagpur-II, Ambigeria, Madpur, Paschim Medinipur, 721149, West Bengal, India.*

[d]*Department of Chemistry, Sri Ramkrishna Sarada Vidyamahapitha, Kamarpukur, West Bengal, 712612, India.*

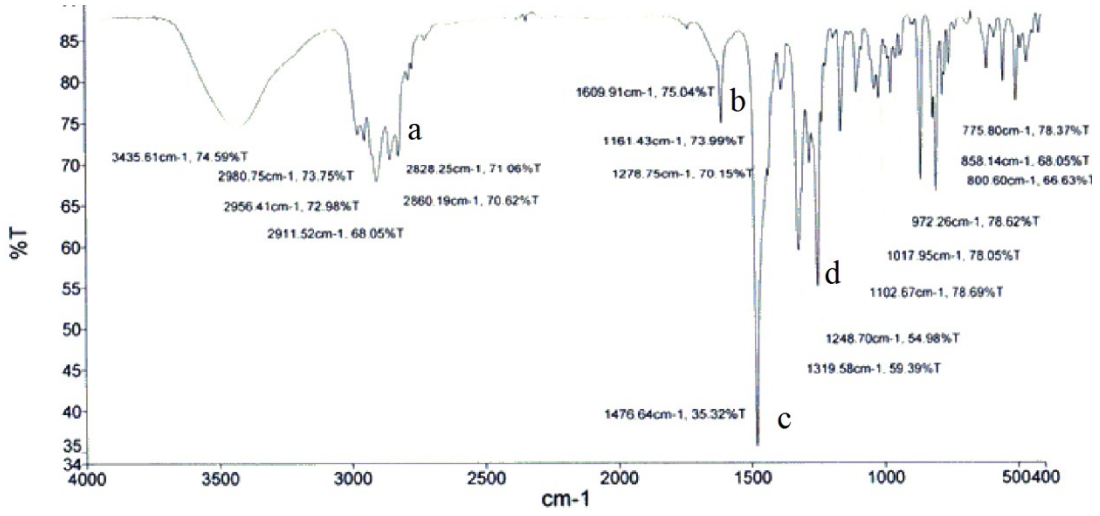

Fig. S1. Representative IR spectrum of dinuclear complex of H_2L^1. [ν(C–H) = 2828–2980 cm^{-1} (a), ν(C=C) = 1609 &1476 cm^{-1}(b & c), ν(C–O/phenolate) = 1248 cm^{-1} (d)]

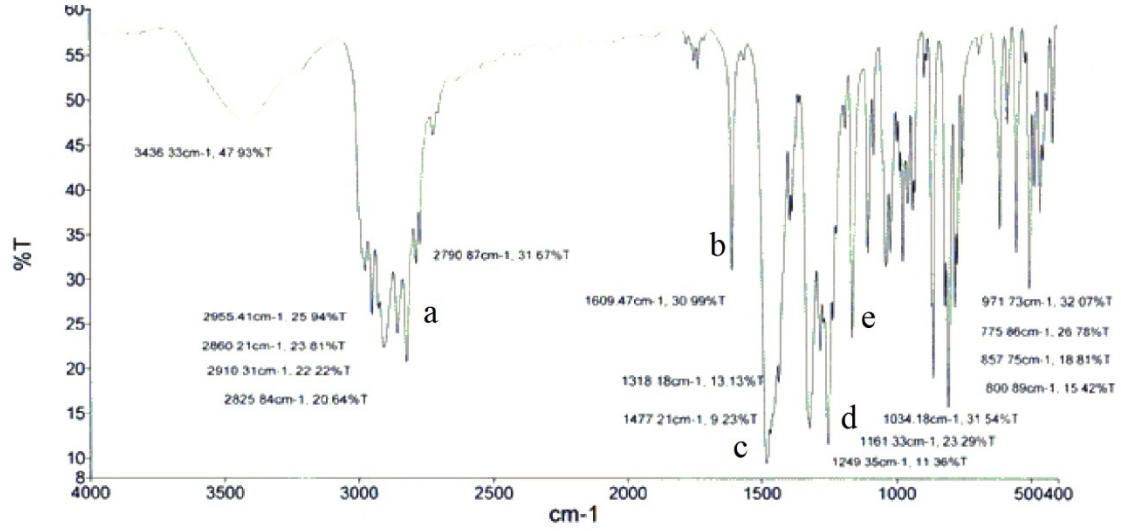

Fig. S2. Representative IR spectrum of dinuclear complex of H_2L^2. [ν(C–H) = 2790–2965 cm^{-1} (a), ν(C=C) = 1609 &1477 cm^{-1}(b & c), ν(C–O/phenolate) = 1248 cm^{-1}(d), ν(C–N) = 1161 cm^{-1} (e)]

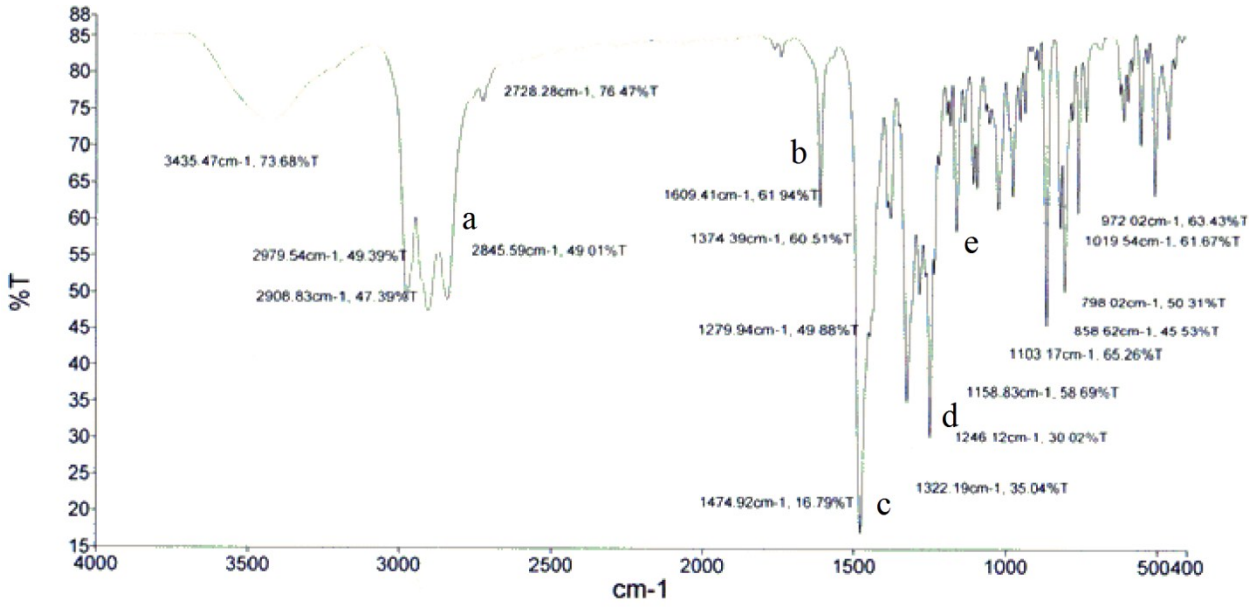

Fig. S3. Representative IR spectrum of dinuclear complex of H_2L^3. [ν(C–H) = 2845–2979 cm^{-1} (a), ν(C=C) = 1609 &1474 cm^{-1}(b & c), ν(C–O/phenolate) = 1246 cm^{-1}(d), ν(C–N) = 1158 cm^{-1} (e)]

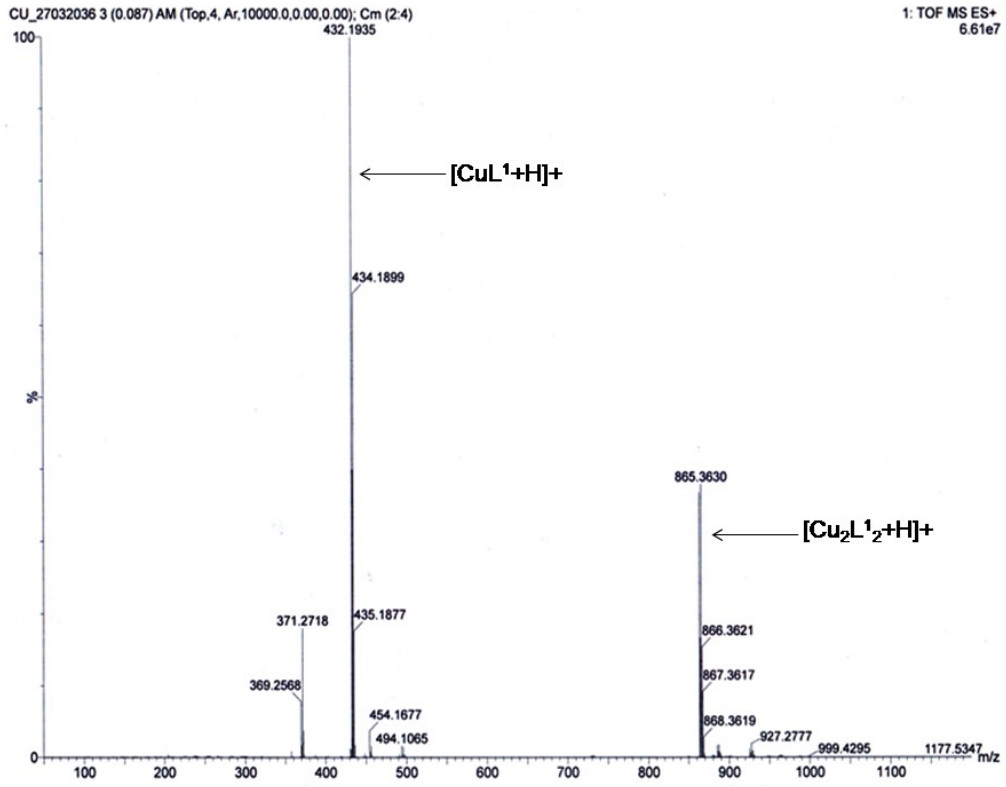

Fig. S4. Representative ESI mass spectrum of dinuclear complex of H_2L^1.

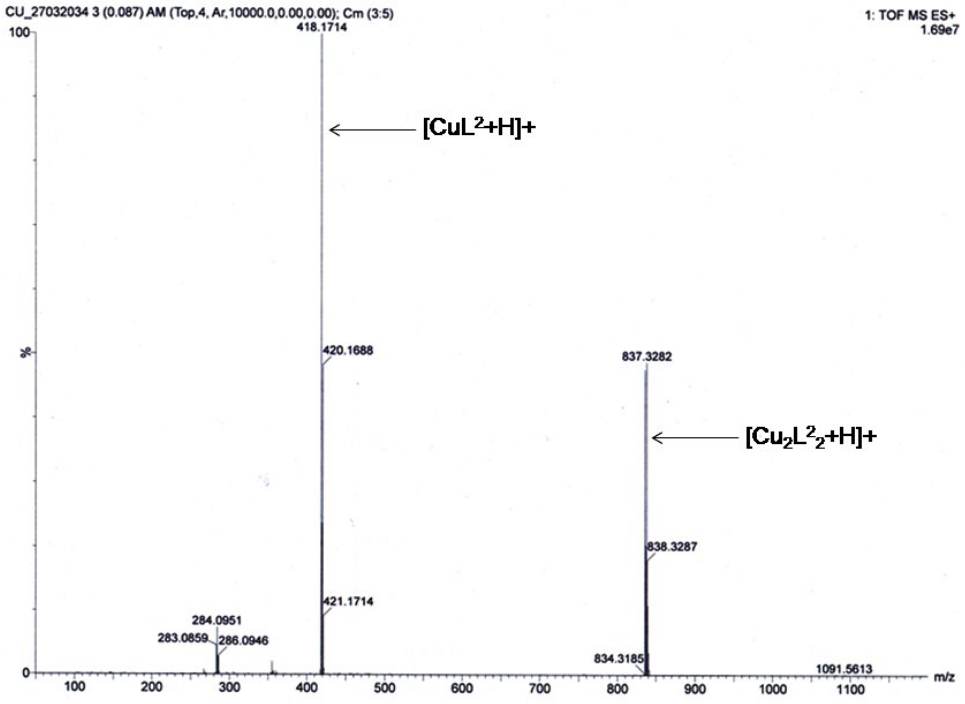

Fig. S5. Representative ESI mass spectrum of dinuclear complex of H_2L^2.

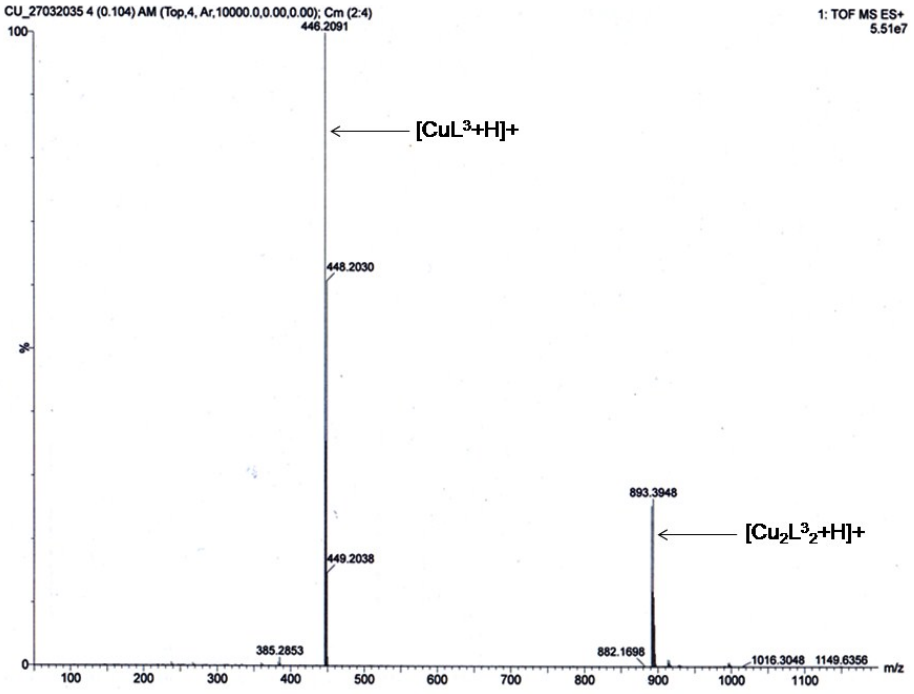

Fig. S6. Representative ESI mass spectrum of dinuclear complex of H_2L^3.

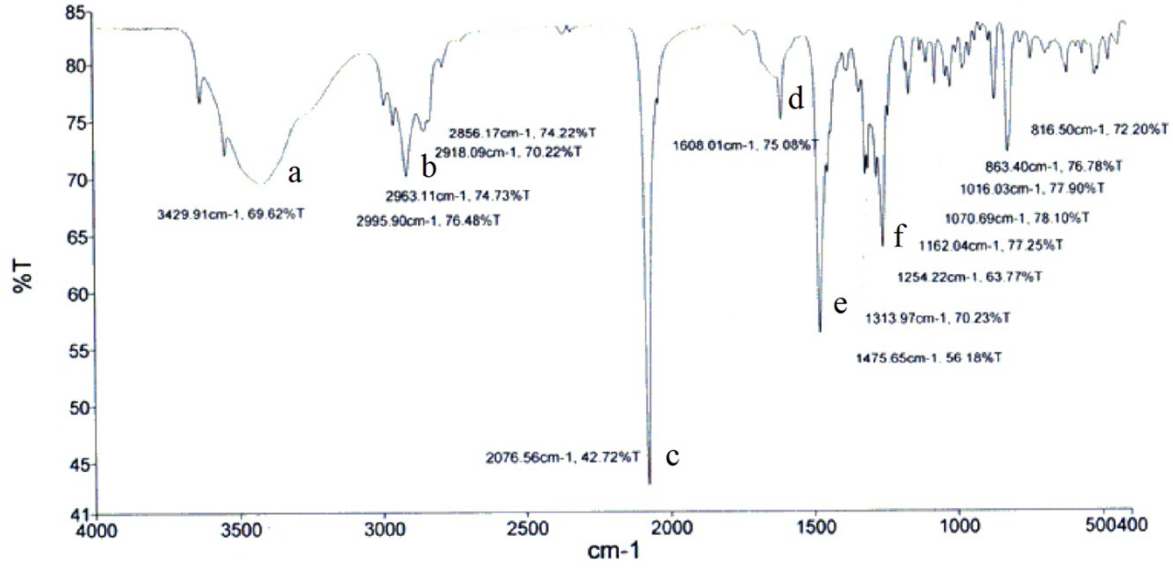

Fig. S7. Representative IR spectrum of complex of **1.** [ν(O–H) = 3429 cm^{-1} (a), ν(C–H) = 2856–2995 cm^{-1}(b), ν(N_3^-)= 2076 cm^{-1}(c), ν(C=C)=1608 &1475 cm^{-1}(d & e), ν(C–O/phenolate) = 1254 cm^{-1}(f)]

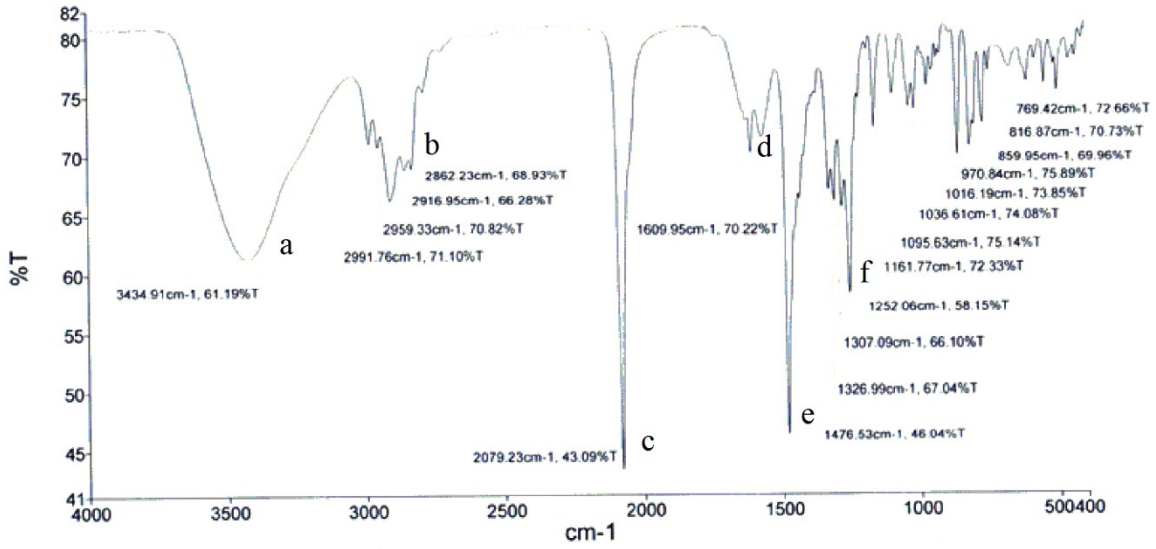

Fig. S8. Representative IR spectrum of complex of **2.** [ν(O–H) = 3434 cm^{-1} (a), ν(C–H) = 2862–2991 cm^{-1}(b), ν(N_3^-)= 2079 cm^{-1}(c), ν(C=C)=1609 &1476 cm^{-1}(d & e), ν(C–O/phenolate) = 1252 cm^{-1}(f)]

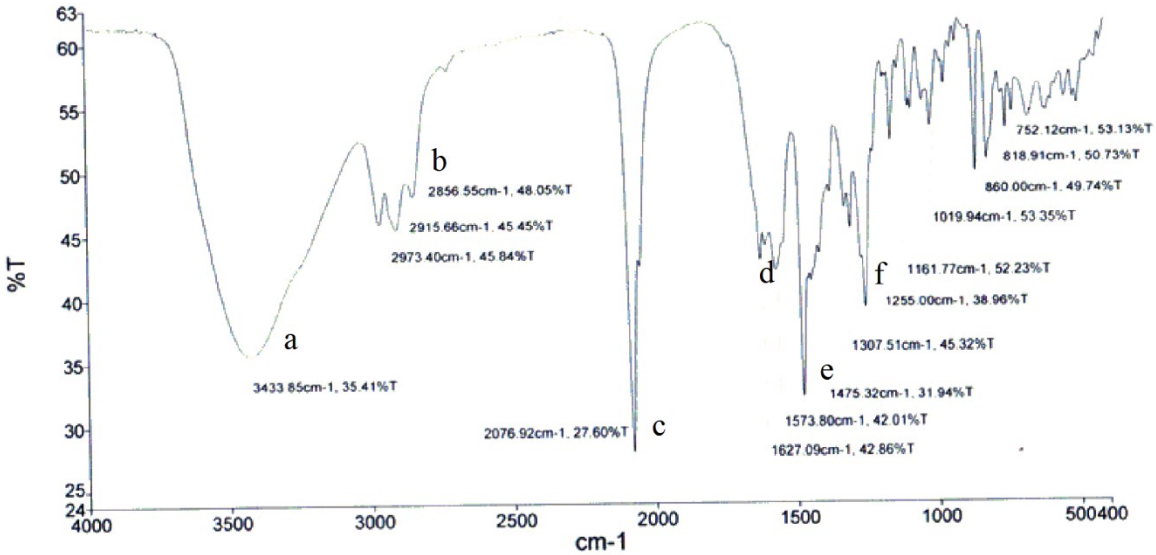

Fig. S9. Representative IR spectrum of complex of **3.** [ν(O–H) = 3433 cm^{-1} (a), ν(C–H) = 2856–2973 cm^{-1}(b), ν(N_3^-)= 2076 cm^{-1}(c), ν(C=C)=1610 &1475 cm^{-1}(d & e), ν(C–O/phenolate) = 1255 cm^{-1}(f)]

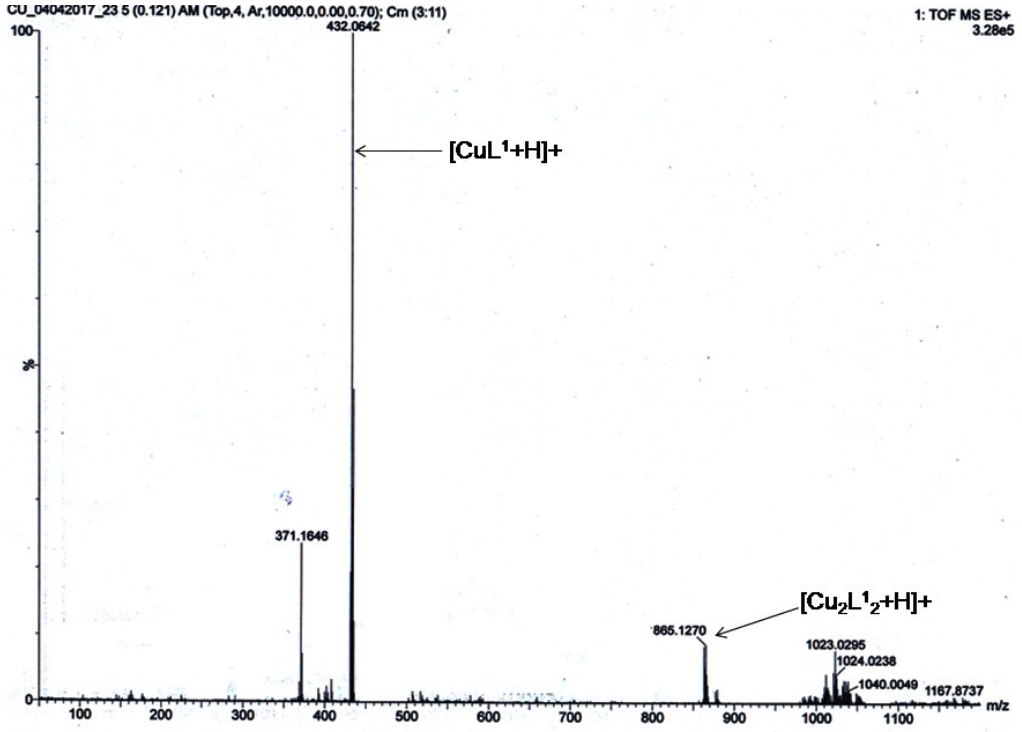

Fig. S10. Representative ESI mass spectrum of complex **1.**

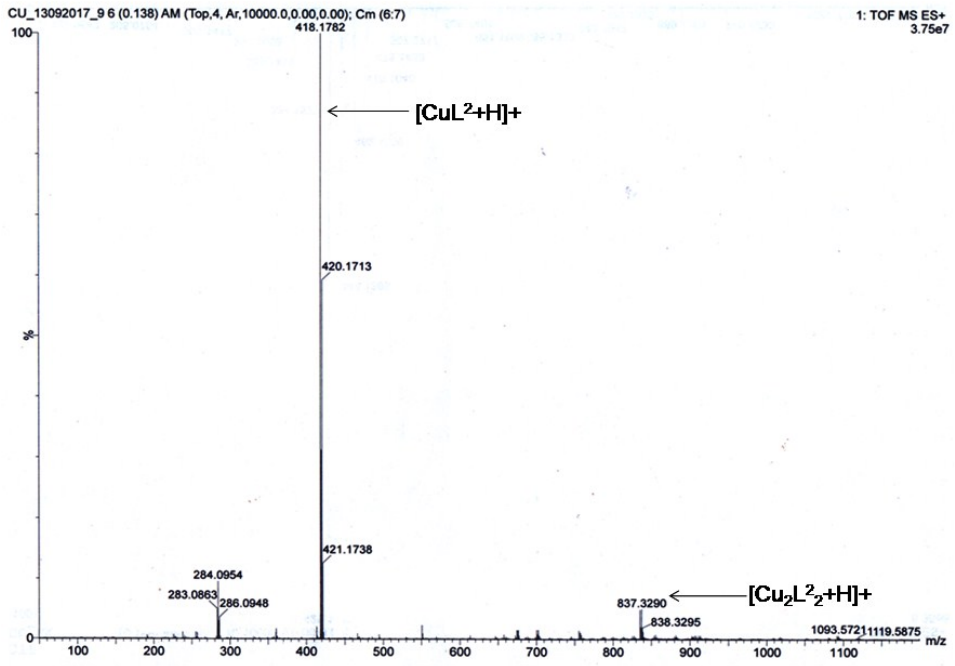

Fig. S11. Representative ESI mass spectrum of complex **2.**

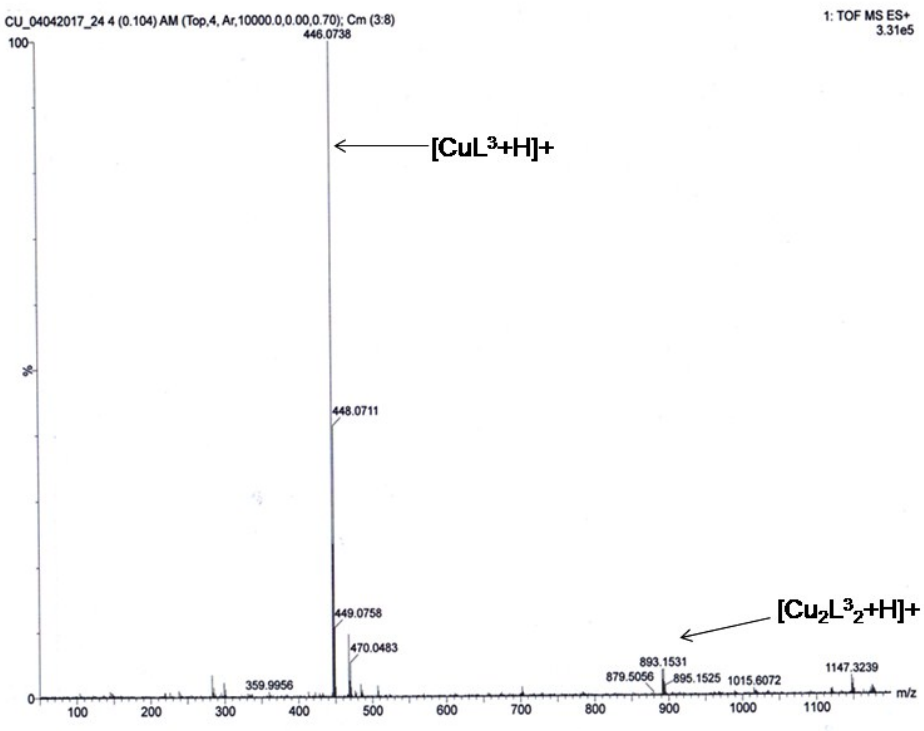

Fig. S12. Representative ESI mass spectrum of complex **3.**

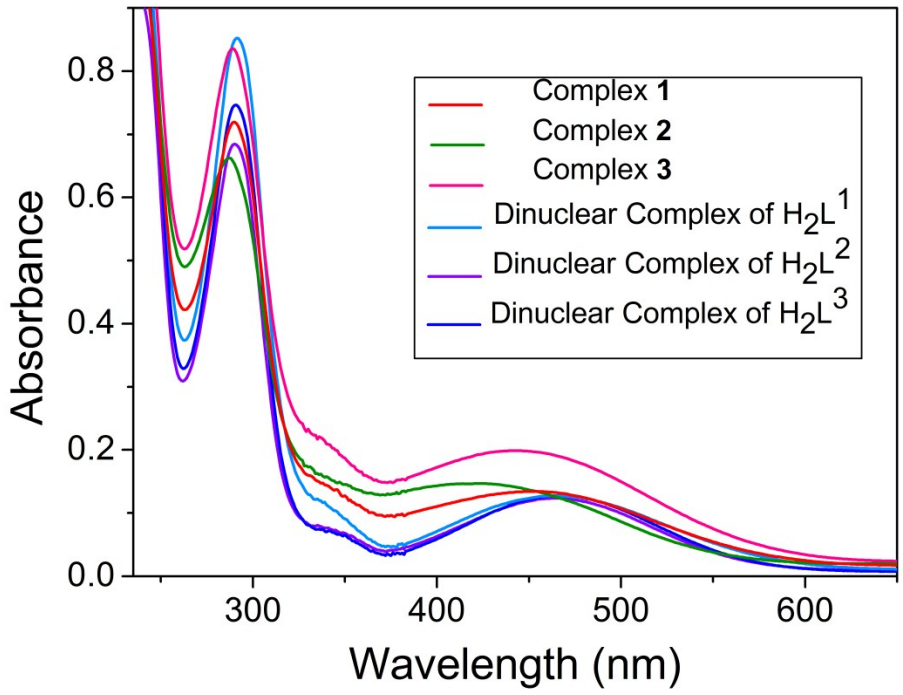

Fig. S13. Electronic spectra of dinuclear complexes and complexes **1-3** in methanol solvent.

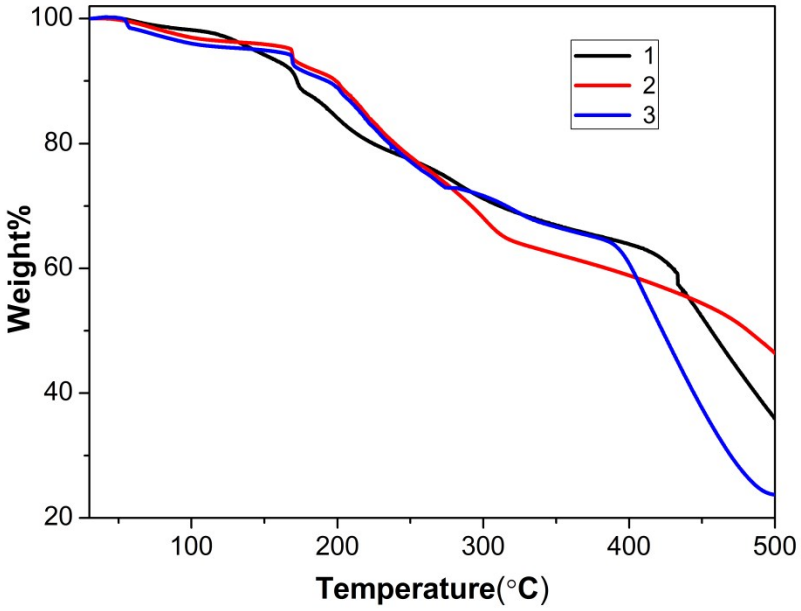

Fig. S14. Thermogravimetric analysis (TGA) plot for complexes **1-3.**

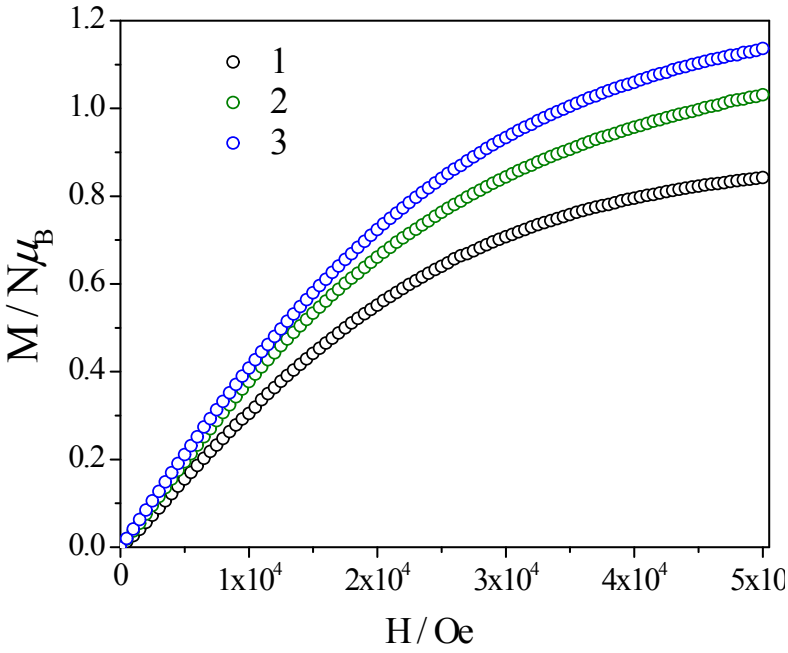

Fig. S15. Field dependence of molar magnetizations for compounds **1-3** at 2 K.

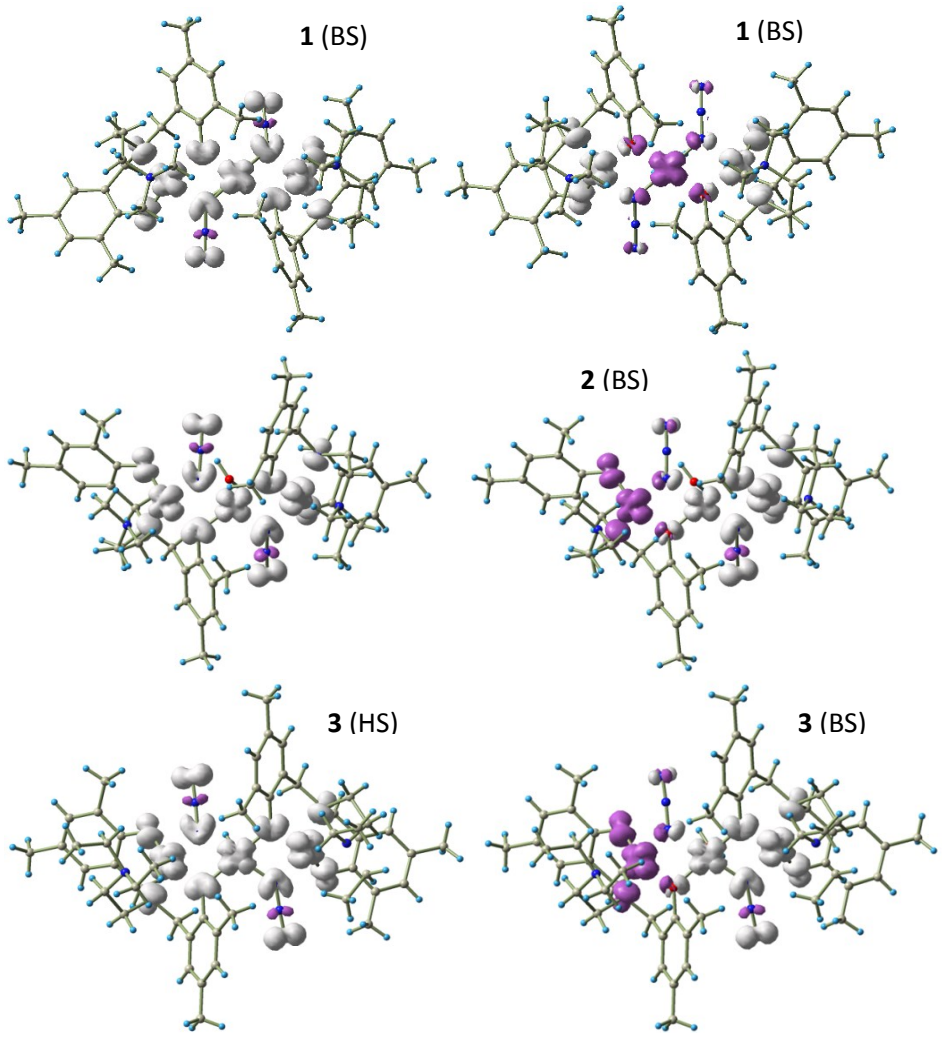

Fig. S16. The calculated isodensity surfaces for highspin (left) and broken symmetry (right) state of complex **1** (upper panel), complex **2** (middle panel)and complex **3** (lower panel) with surface cutoff value 0.004 e/Å^3.Positive and negative spin densities are represented by gray and purple surfaces respectively.

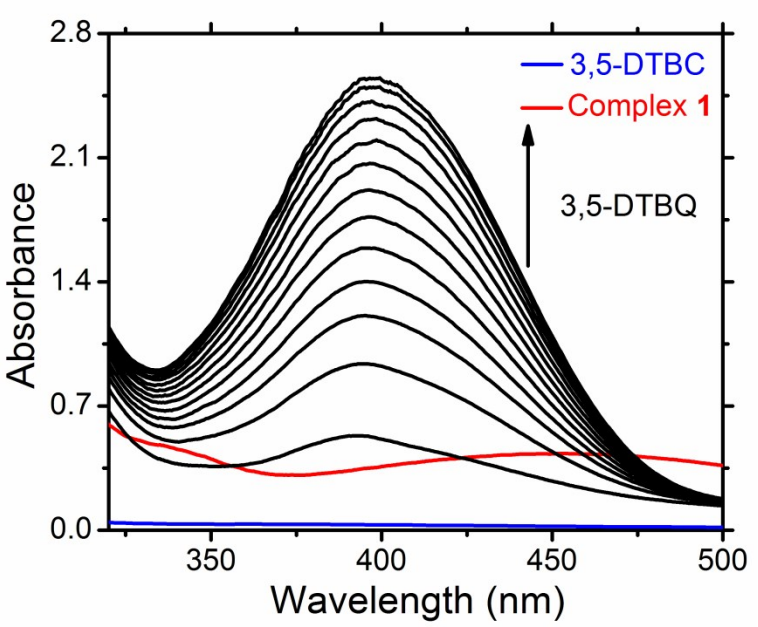

Fig. S17. Increase of absorption spectra after addition of 100 equiv of 3,5-DTBC to a methanolic solution of complex **1**. These spectra were recorded at 5 min intervals.

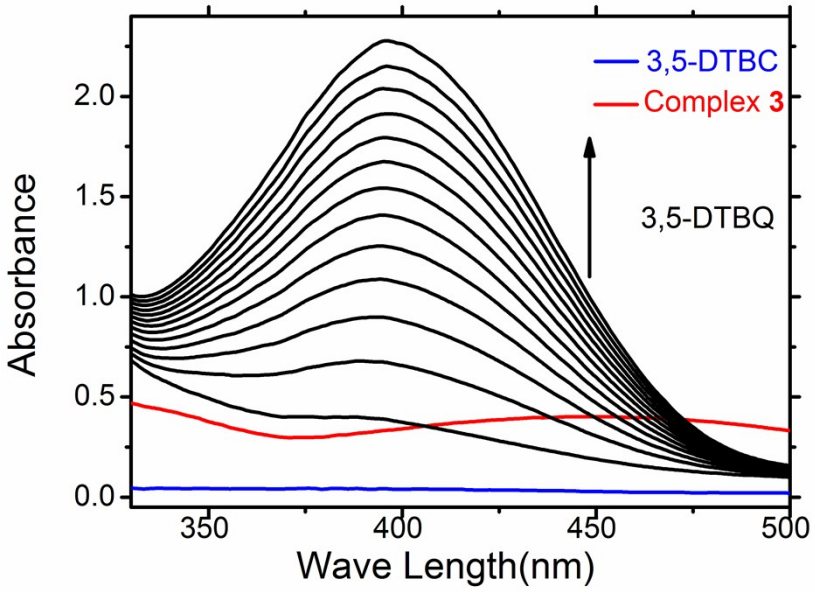

Fig. S18. Increase of absorption spectra after addition of 100 equiv of 3,5-DTBC to a methanolic solution of complex **3**. These spectra were recorded at 5 min intervals.

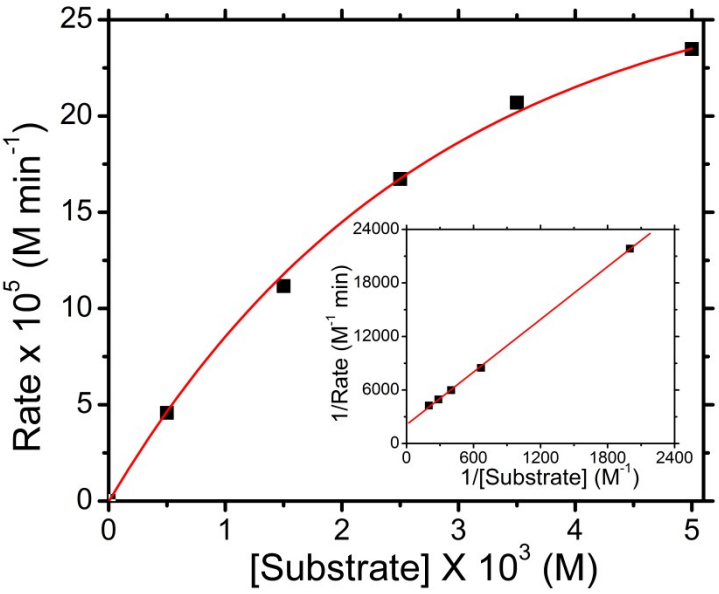

Fig. S19. Plot of the rate *vs*. substrate concentration for complex **1**. The inset shows the corresponding Lineweaver - Burk plot.

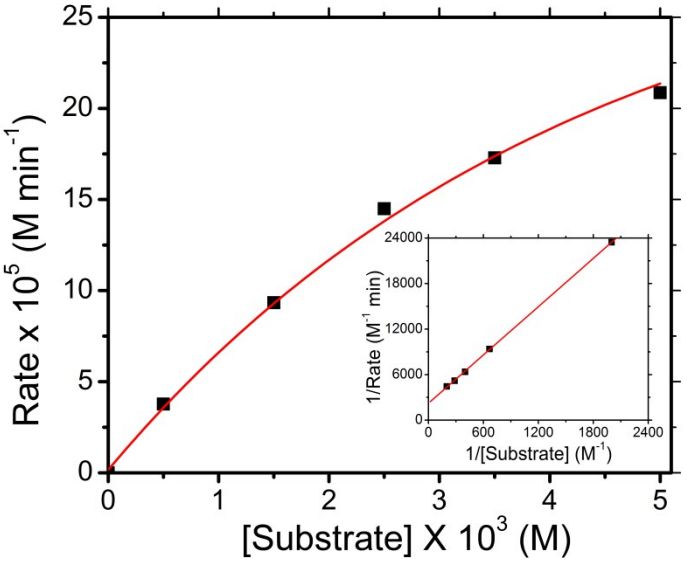

Fig. S20. Plot of the rate *vs*. substrate concentration for complex **3**. The inset shows the corresponding Lineweaver - Burk plot.

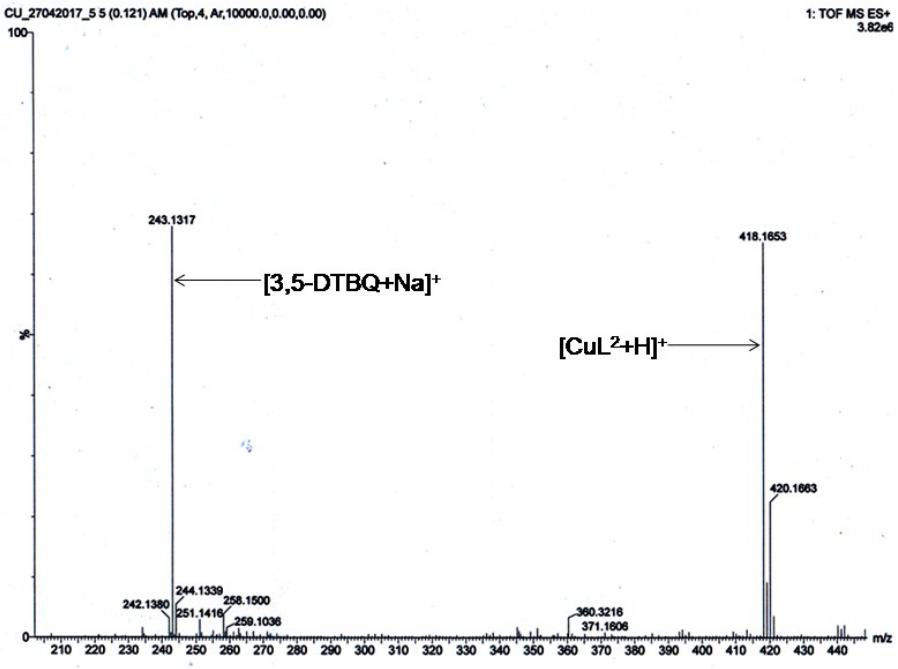

Fig. S21. Representative ESI mass spectrum of complex **2** in CH_3OH solvent after addition of 3,5-DTBC.

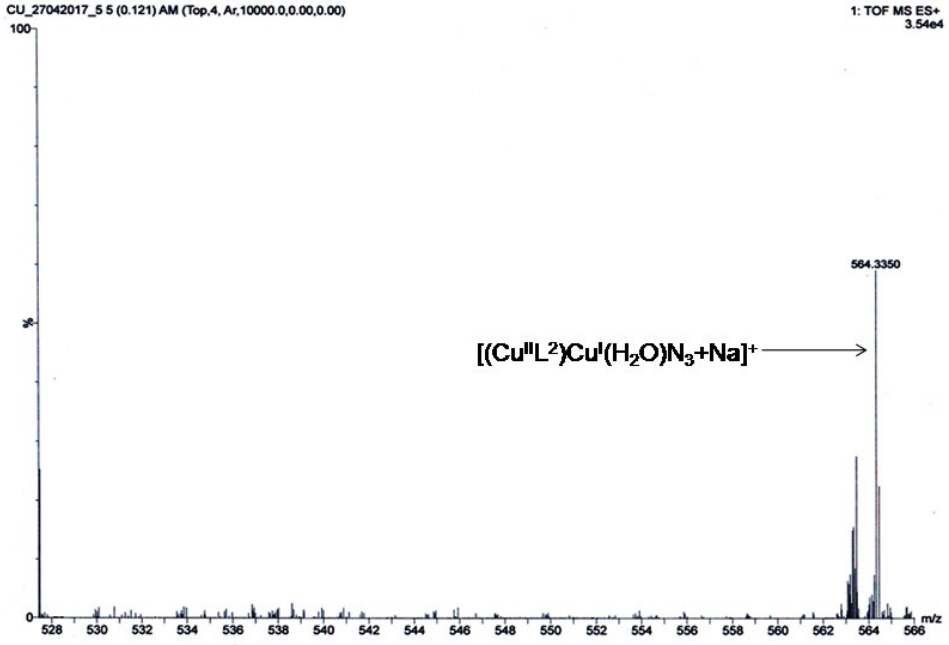

Fig. S22. Representative ESI mass spectrum of complex **2** in CH_3OH solvent after addition of 3,5-DTBC (Expanded from 528 to 566).

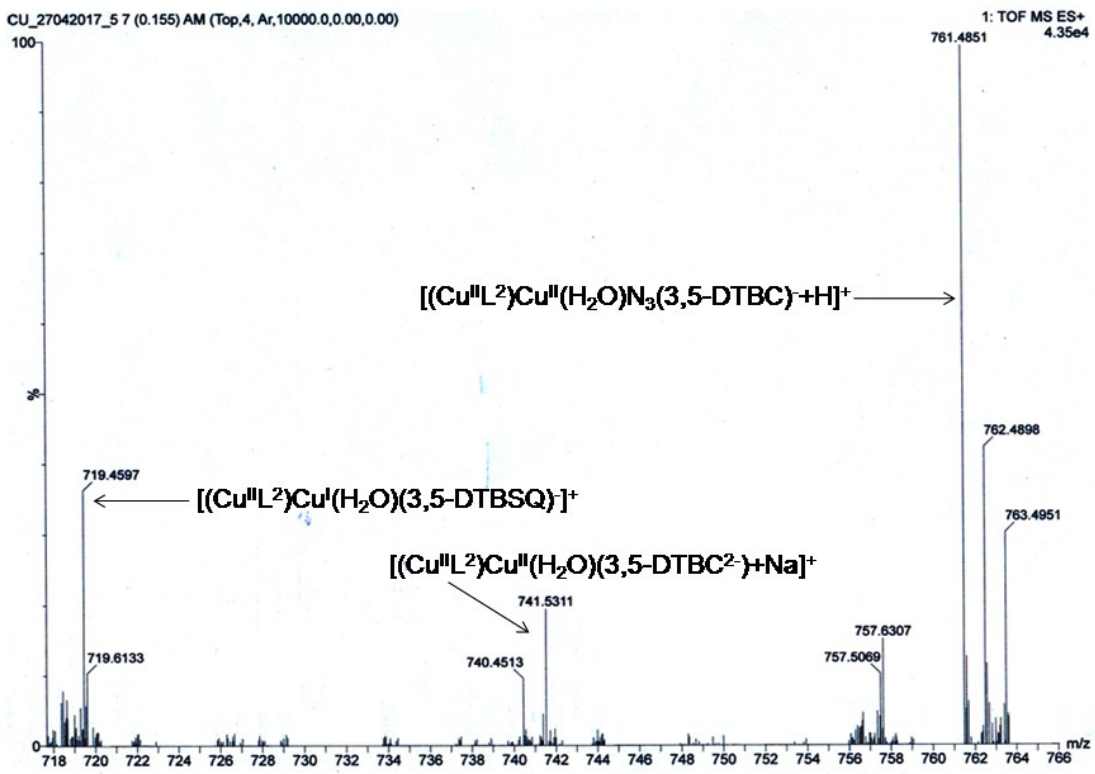

Fig. S23. Representative ESI mass spectrum of complex **2** in CH_3OH solvent after addition of 3,5-DTBC (Expanded from 718 to 766).

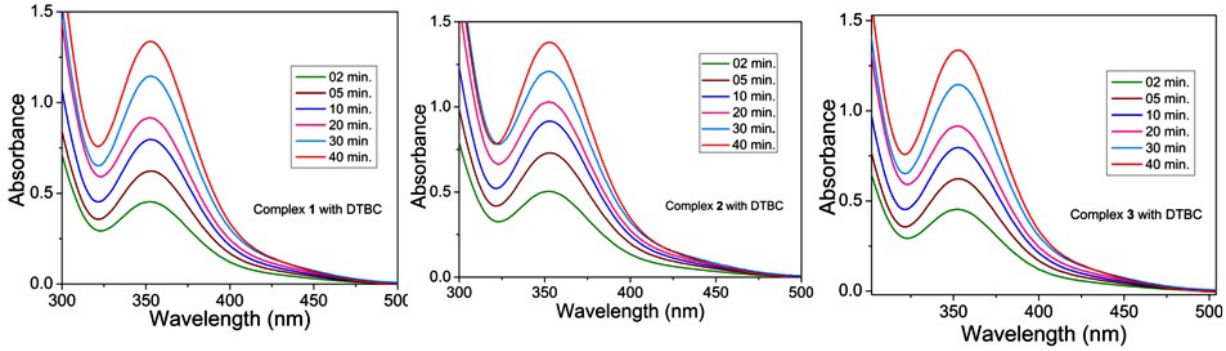

Fig. S24. Increase of the absorption band at around 353 nm during the estimation of H_2O_2 iodometrically. The spectra were recorded at different time interval for complexes **1-3.**

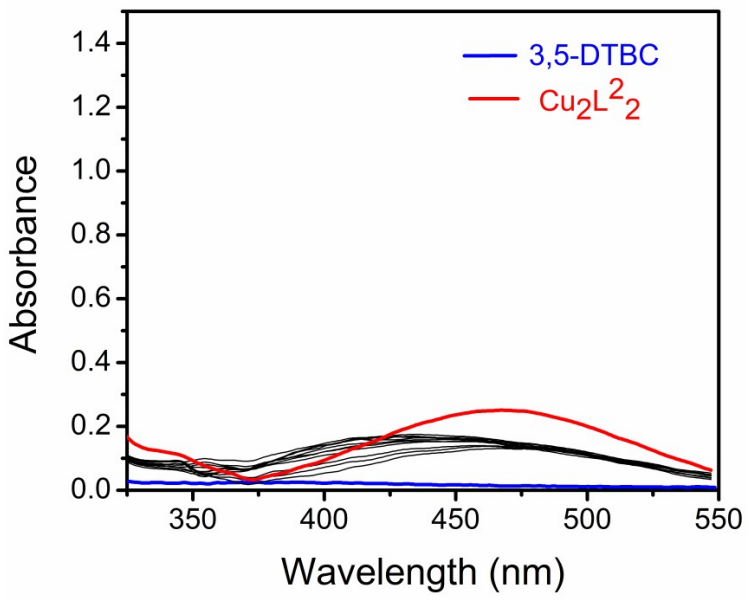

Fig. S25. Absorption spectra after addition of 100 equiv of 3,5-DTBC to a methanolic solution of dinuclear complex of H_2L^2. These spectra were recorded at 5 min intervals upto 1 hr.

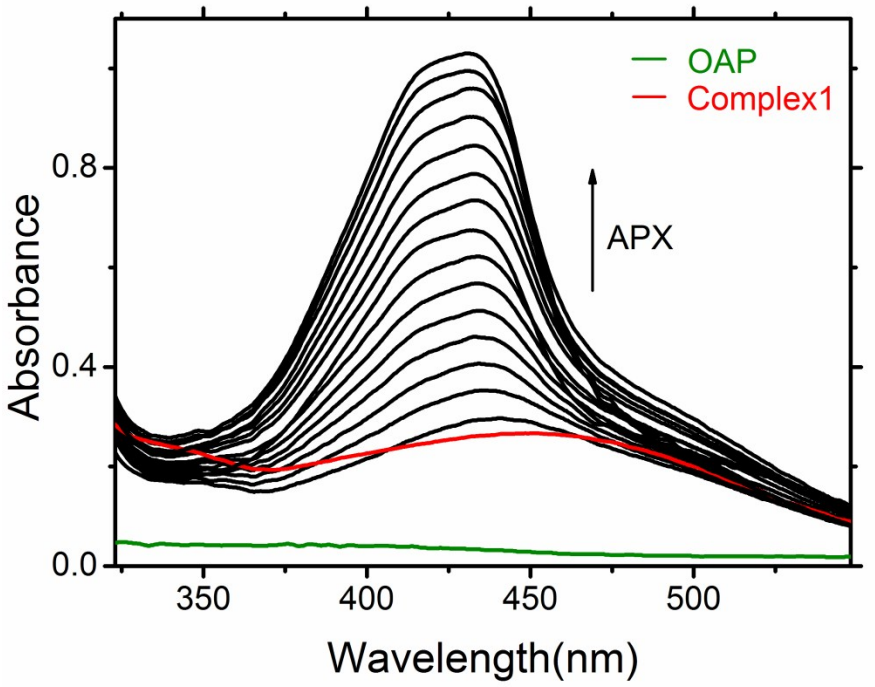

Fig. S26. Increase of the APX band at 432 nm after the addition of 100 equiv of OAP to a methanol solution with complex **1**. The spectra were recorded at 5 min intervals.

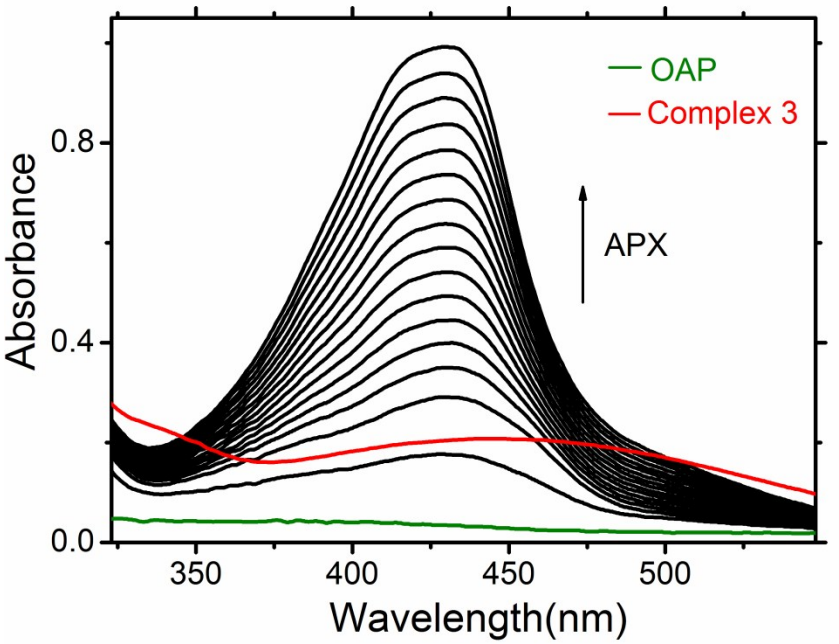

Fig. S27. Increase of the APX band at 432 nm after the addition of 100 equiv of OAP to a methanol solution with complex **3**. The spectra were recorded at 5 min intervals.

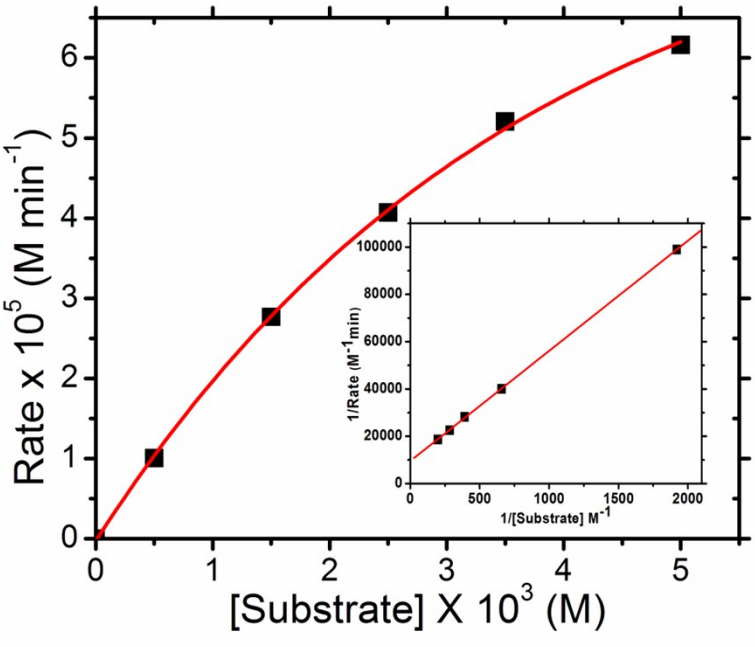

Fig. S28. Plot of the rate *vs* substrate concentration for complex **1**. Inset shows the corresponding Lineweaver−Burk plot.

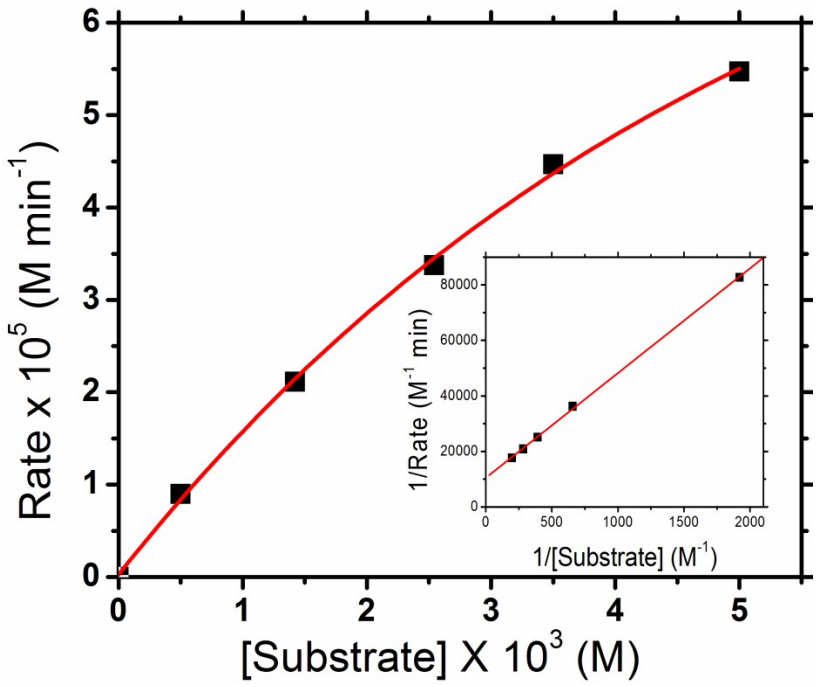

Fig. S29. Plot of the rate *vs* substrate concentration for complex **3**. Inset shows the corresponding Lineweaver−Burk plot.

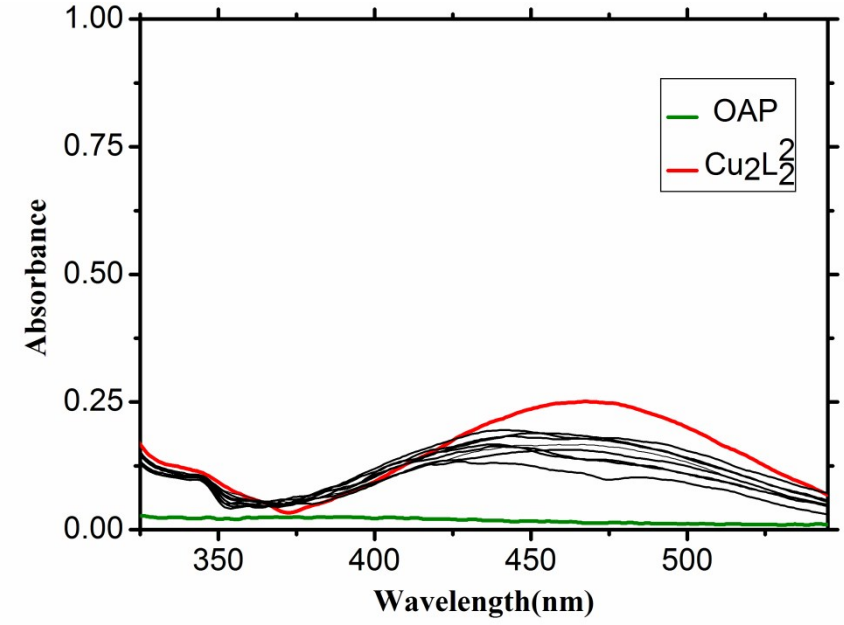

Fig. S30. UV-VIS spectra after addition of 100 equiv of OAP to a methanolic solution of Dinuclear complex of H_2L^2. These spectra were recorded at 5 min intervals upto 1 hr.

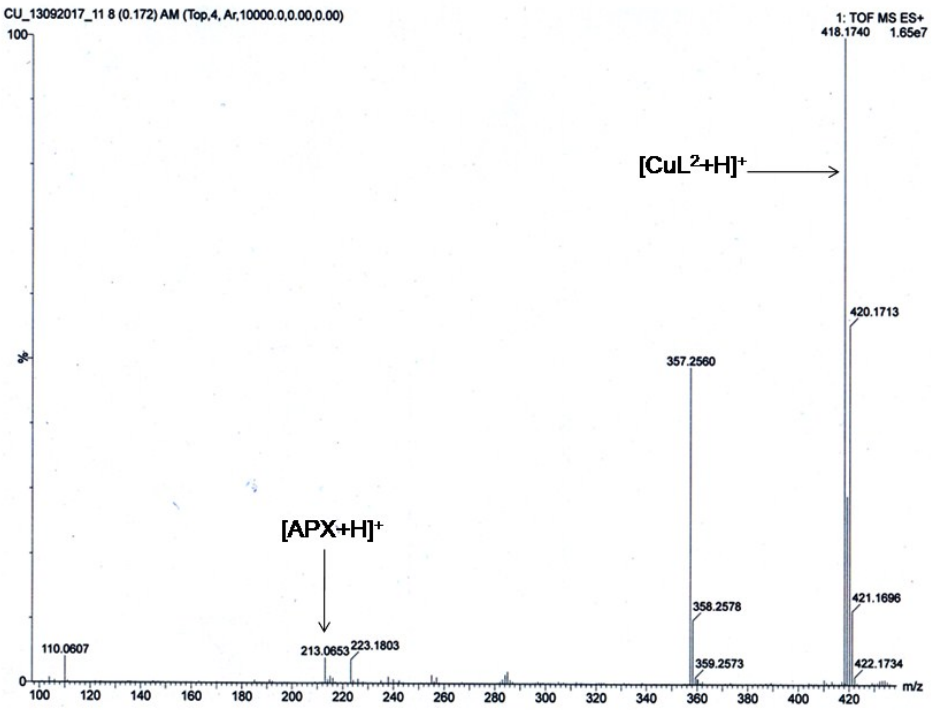

Fig. S31. Representative ESI mass spectrum of complex **2** in CH_3OH solvent after addition of OAP.

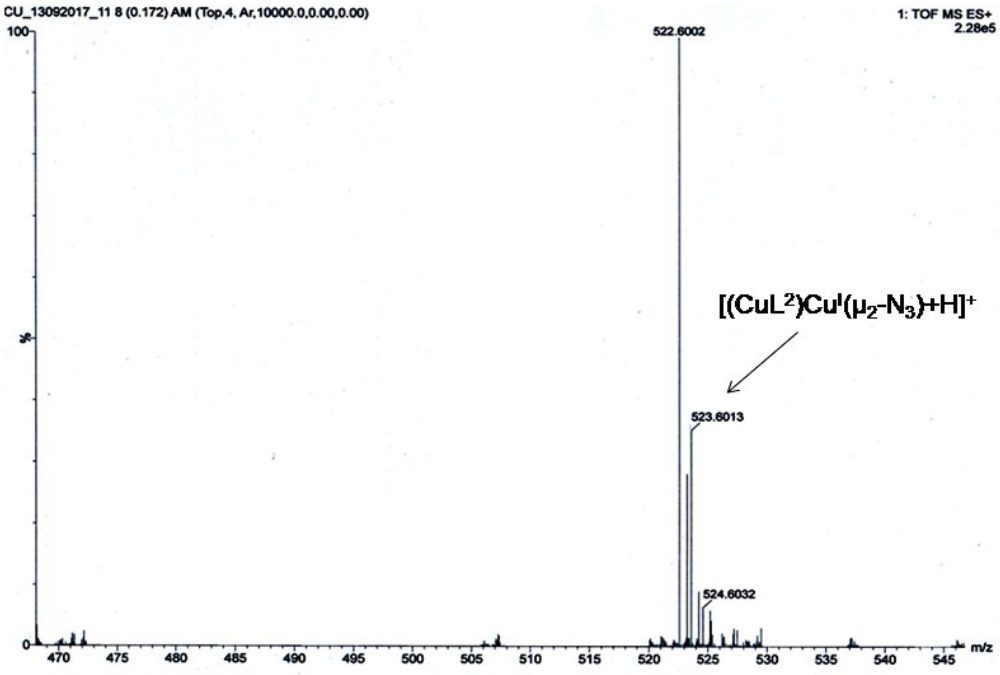

Fig. S32. Representative ESI mass spectrum of complex **2** in CH_3OH solvent after addition of OAP (Expanded from 470 to 545).

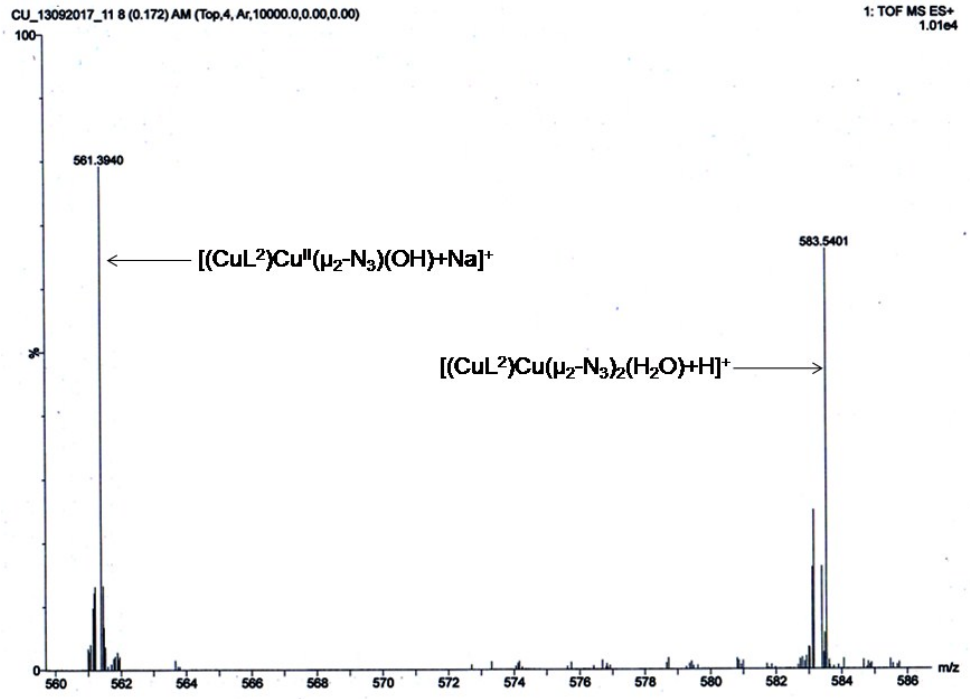

Fig. S33. Representative ESI mass spectrum of complex **2** in CH_3OH solvent after addition of OAP (Expanded from 560 to 586).

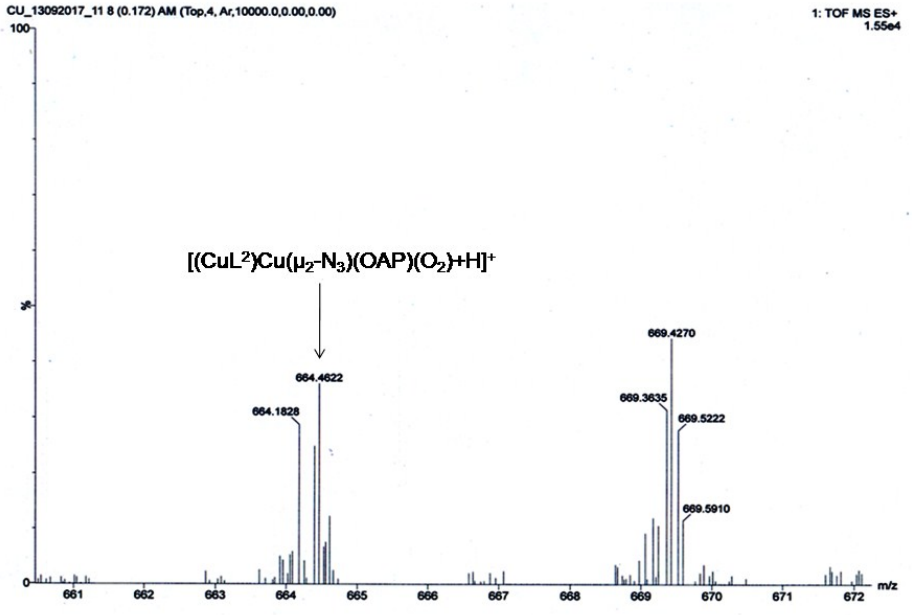

Fig. S34. Representative ESI mass spectrum of complex **2** in CH_3OH solvent after addition of OAP (Expanded from 661 to 672).

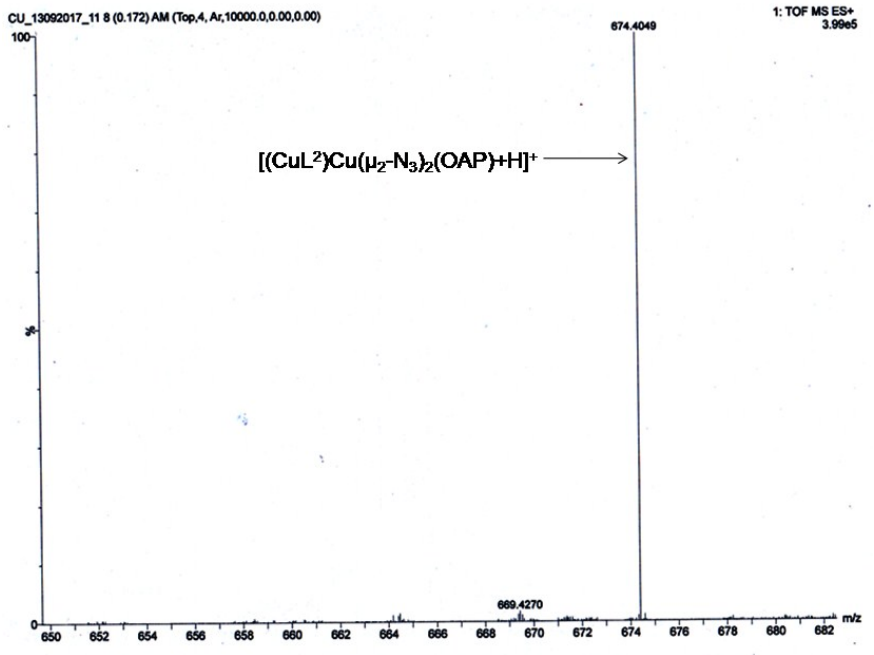

Fig. S35. Representative ESI mass spectrum of complex **2** in CH_3OH solvent after addition of OAP (Expanded from 650 to 682).

Table S1. Selected bond lengths and bond angles for complexes **1 -3**.

Bond distances (Å)				
Parameters	**1**	**Parameters**	**2**	**3**
Cu1—O1	1.903(3)	Cu1—O1	1.897(3)	1.907(2)
Cu1—O2	1.978(2)	Cu1—O2	1.975(3)	1.979(2)
Cu1—N1	2.054(3)	Cu1—N1	2.044(3)	2.026(3)
Cu1—N2	2.242(3)	Cu1—N2	2.296(4)	2.311(7)
Cu1—N3#	2.035(3)	Cu1—N5	2.016(3)	1.998(3)
Cu2—O2	1.945(2)	Cu2—O2	1.943(3)	1.924(2)
Cu2—O2#	1.945(2)	Cu2—O3	1.929(3)	1.922(2)
Cu2—N3	1.963(3)	Cu2—N5	1.981(3)	1.982(3)
Cu2—N3#	1.963(3)	Cu2—N8	1.983(3)	1.968(3)
Cu2—O3	2.406(5)	Cu2—O5	2.613(5)	2.388(4)
Cu1#—N3	2.035(3)	Cu3—O3	1.968(3)	1.964(2)
		Cu3—O4	1.900(3)	1.900(3)
		Cu3—N3	2.063(3)	2.030(3)
		Cu3—N4	2.326(3)	2.329(11)
		Cu3—N8	2.053(3)	2.005(3)
Bond Angles (deg)				
Parameters	**1**	**Parameters**	**2**	**3**
O1—Cu1—O2	158.09(11)	O1—Cu1—O2	156.53(12)	158.37(10)
O1—Cu1—N3#	88.15(12)	O1—Cu1—N5	89.73(12)	90.31(12)
O2—Cu1—N3#	76.03(10)	O2—Cu1—N5	76.65(11)	76.57(11)
O1—Cu1—N1	95.61(12)	O1—Cu1—N1	96.10(12)	95.39(11)
O2—Cu1—N1	94.23(10)	O2—Cu1—N1	94.09(11)	92.86(11)
N3#—Cu1—N1	159.33(12)	N5—Cu1—N1	167.62(13)	162.93(12)
O1—Cu1—N2	100.48(13)	O1—Cu1—N2	105.13(15)	98.41(14)
O2—Cu1—N2	96.97(11)	O2—Cu1—N2	97.07(13)	102.38(11)
N3#—Cu1—N2	99.14(12)	N5—Cu1—N2	106.12(14)	111.65(2)
N1—Cu1—N2	100.13(12)	N1—Cu1—N2	82.94(12)	83.46(17)
O2—Cu2—O2#	162.64(15)	O2—Cu2—O3	168.13(11)	167.28(10)
O2—Cu2—N3	101.89(11)	O2—Cu2—N8	102.46(12)	102.35(11)
O2#—Cu2—N3	78.47(11)	O3—Cu2—N5	102.00(16)	102.22(11)
O2—Cu2—N3#	78.47(11)	O3—Cu2—N8	78.74(12)	77.92(11)
O2#—Cu2—N3#	101.89(11)	O3—Cu2—N5	102.05(11)	102.22(11)
N3—Cu2—N3#	177.68(19)	N5—Cu2—N8	173.28(15)	176.95(13)
O2—Cu2—O3	98.68(7)	O2—Cu2—O5	92.18(2)	97.66(13)
O2#—Cu2—O3	98.68(7)	O3—Cu2—O5	99.69(15)	95.06(13)
N3—Cu2—O3	88.84(10)	N8—Cu2—O5	84.08(2)	89.56(14)
N3#—Cu2—O3	88.84(10)	N5—Cu2—O5	89.3(2)	87.39(13)
Cu1—O2—Cu2	100.09(10)	Cu1—O2—Cu2	97.28(11)	97.49(10)
Cu1—N3—Cu2	97.54(13)	Cu1—N5—Cu2	94.74(13)	94.99(13)
		Cu2—O3—Cu3	98.82(11)	98.58(11)
		Cu2—N8—Cu3	94.31(12)	95.68(12)
		O4—Cu3—O3	162.14(12)	159.72 (15)
		O4—Cu3—N8	90.20(13)	90.37(12)
		O3—Cu3—N8	76.19(12)	76.08(11)
		O4—Cu3—N3	95.50(13)	95.70(11)
		O3—Cu3—N3	93.31(12)	93.13(11)
		N8—Cu3—N3	158.18(2)	163.20(13)
		O4—Cu3—N4	100.89(13)	99.2(3)
		O3—Cu3—N4	95.71(12)	101.5(3)
		N8—Cu3—N4	117.56(12)	109.1(3)
		N3—Cu3—N4	81.92(12)	85.5(3)

(#) 2-x, y, 0.5-z.

Table S2. Hydrogen bonding parameters for complexes **1**-**3**.

Compound	D–H•••A	D-H, (Å)	H•••A, (Å)	D•••A, (Å)	∠D–H•••A, (deg)
1	O3–H3W···O4	0.83(5)	2.02(5)	2.808(4)	159(5)
	O4–H4···O1	0.82	1.93	2.747(5)	179
2	O7–H7···O4	0.82	1.91	2.725(7)	170
3	O5–H5A···O6	0.94(3)	1.78(3)	2.694(6)	162(3)
	O5–H5B···O7	0.93(4)	1.86(4)	2.780(5)	167(4)
	O6–H6···O4	0.91(6)	1.78(6)	2.693(5)	177(4)
	O7–H7···O1	0.82(4)	1.84(4)	2.654(4)	170(4)

Table S3. Magnetic parameters for complexes **1**–**3**.

Compounds	g	J / cm^{-1}	θ / K	R
1	2.13 ±0.06	−64.42 ±0.20	0.07± 0.02	1.5×10^{-5}
2	2.06 ±0.04	−9.60 ±0.07	−0.30 ±0.03	2.0×10^{-5}
3	2.07 ±0.06	−4.54±0.04	0.45±0.02	1.7×10^{-5}

Table S4. Magnetic and structural parameters for complexes **1**–**3**.

Complexes	∠ Cu−O−Cu (°)	∠ Cu−N−Cu (°)	Hinge distortion (°)	$J_{Exp.}$/cm^{-1}	$J_{DFT.}$/ cm^{-1}
1	100.09	97.54	27.16	−64.42 ±0.20	J_1=J_2= −68.07
2	97.28 98.82	94.74 94.31	35.72 33.38	−9.60 ±0.07	J_1= +2.84 J_2= −13.22 $J_{av.}$ = −5.19
3	97.49 98.58	94.99 95.68	33.35 34.96	−4.54 ±0.04	J_1= −0.71 J_2= −3.68 $J_{av.}$ = −2.19
VAJBUF	97.10	97.16	25.15	−9.86	---
VAJCAM	97.07	97.39	24.78	−19.98	---
ZEGZES	100.93	97.26	5.43	−31.54	---
VAJBOZ	100.79	96.53	20.26	−11.6	---

Table S5. Mulliken spin densities(in au) for high-spin (HS) state of structures **1**–**3**.

Selected atoms	Complex **1**	Complex **2**	Complex **3**
Cu1 *(terminal)*	0.60855	0.60228	0.60239
Cu2 *(central)*	0.61059	0.59133	0.5988
Cu3 *(terninal)*	0.60855	0.60424	0.6034
O2 *(μ-1,1-phenoxido)*	0.11465	0.1266	0.12111
O3 *(μ-1,1-phenoxido)*	0.11465	0.11055	0.11889
O5 *(water)*	1.58×10^{-4}	-3.1×10^{-5}	2.63×10^{-4}
N5*(azide)*	0.10648	0.10689	0.1031
N6*(azide)*	−0.02656	−0.03091	−0.0281
N7*(azide)*	0.12336	0.13451	0.13336
N8*(azide)*	0.10649	0.10039	0.10014
N9*(azide)*	−0.02656	−0.03193	−0.02837
N10*(azide)*	0.12336	0.14085	0.13343
N1 *(coordinating)*	0.09322	0.0917	0.09979
N2 *(coordinating)*	1.32×10^{-4}	0.00296	4.68×10^{-4}
N3 *(coordinating)*	0.09322	0.10123	0.10115
N4 *(coordinating)*	1.34×10^{-4}	-2.32×10^{-4}	3.65×10^{-4}
O1 *(coordinating)*	0.12478	0.129	0.12111
O4 *(coordinating)*	0.12479	0.11769	0.11889

Table S6. Kinetic Parameters for the Oxidation of 3,5-DTBC Catalyzed by Complexes **1-3**.

Complexes	**V_{max} (M min^{-1})**	**Std. error**	**K_M (M)**	**Std. error**	**k_{cat} (h^{-1})**
1	4.74×10^{-4}	2.40×10^{-5}	46.63×10^{-4}	5.21×10^{-5}	568.8
2	4.52×10^{-4}	1.35×10^{-5}	47.96×10^{-4}	3.06×10^{-5}	542.1
3	4.17×10^{-4}	1.99×10^{-5}	50.43×10^{-4}	4.92×10^{-5}	500.4

Table S7. Catecholase activity data for some Cu(II) complexes .

Complex	Solvent used	k_{cat} (h^{-1})	References
$[Cu_3L^1_2(N_3)_2(H_2O)(CH_3OH)]$	CH_3OH	568.8	This work
$[Cu_3L^2_2(N_3)_2(H_2O)(CH_3OH)_2]$	CH_3OH	542.1	This work
$[Cu_3L^3_2(N_3)_2(H_2O)(CH_3OH)_2]$	CH_3OH	500.4	This work
$[Cu_3(L^4)(\mu\text{-}OAc)](ClO_4)_2$	CH_3OH/H_2O	80.28	39(a)
$[Cu_3(\mu\text{-}OH)(dppi)_3(L^5)_3]$	THF	16.2	39(b)
$[Cu_3L_2^6](ClO_4)_2 \cdot 5H_2O$	C_2H_5OH/H_2O	9.54	39(c)
$[Cu_3(L^7)(CH_3COO)_3].\ 3H_2O$	CH_3OH	7.5	39(d)
$[Cu_2(H_2L^8)(OH)(H_2O)(NO_3)](NO_3)_3.H_2O]$	CH_3OH	3.24×10^4	40(a)
$[Cu_2(L^9)(N_3)_3]$	CH_3OH	2.88×10^4	40(a)
$[Cu_2(L^{10})(OH)(H_2O)_2](NO_3)_2$	CH_3OH	1.44×10^4	40(a)
$[Cu_2\ (L^{11})(Cl)_2(BF_4)]$	CH_3CN	4700	40(b)
$[Cu_2(L^{12})_2(\text{benzoate})_2]$	CH_3OH	943	40(c)
$[Cu_2(L^{13})_2]$	CH_3OH	720	40(d)
$[Cu_2(L^{12})_2(\text{2-hydroxybenzoate})_2]$	CH_3OH	698	40(c)
$[Cu_2(L^{14})_2(\text{4-hydroxybenzoate})_2][Cu(Htea)_2]$	CH_3OH	553	40(c)
$[Cu_2(L^{15})_2(bba)_2]$	CH_3OH	240	40(e)
$[Cu(HL^{16})(H_2O)(NO_3)](NO_3)_2 \cdot 2H_2O$	CH_3OH	1.44×10^4	40(a)
$[Cu(L^{17})(H_2O)(NO_3)]$	CH_3OH	1.08×10^4	40(a)
$[Cu(L^{18})_2(NCS)]ClO_4$	CH_3OH	1.84×10^4	41(a)
$[Cu(L^{19})Cl_2]$	CH_3OH	1.04×10^4	41(b)
$[Cu(L^{20})(Cl)](BF_4)$	CH_3CN	480	41(c)
$[Cu(L^{21})I_2]$	DMF	63.72	41(d)
$[Cu(H_2L^{22})(ClO_4)]^+$	CH_3OH	58.68	41(e)

[Where L^1 = *N, N*-bis(3,5-dimethyl-2-hydroxybenzyl)-*N′,N′*-dimethyl-1,3-diaminopropane, L^2= *N,N*-bis(3,5-dimethyl-2-hydroxybenzyl)-*N′,N′*-dimethyl-1,2-diaminoethane, L^3 = *N, N*-bis(3,5-dimethyl-2-hydroxybenzyl)-*N′,N′*-diethyl-1,2-diaminoethane,L^4=*N,N′*-bis-(2-pyridyl methyl)-(2-hydroxy-3-carbonyl-5-methylbenzyl)-1,3-propanediamine-2-ol, L^5=hexafluoro acetyl acetonate and dppi=diphenylphosphinate, L^6=*N,N′,N″*–tris(5-pyrazolylmethyl)-cis-1,3,5-triaminocyclohexane,L^7=2,6-diformaldehyde-pyridine, L^8=2,6-bis(*N*-ethylpiperazine-imino methyl)-4-methyl-phenolato, L^9=2,6-bis(*N*-propylmorpholine -iminomethyl)-4-methyl-phenolato, L^{10} = 2,6-bis(*N*-ethylpyrrolidine -iminomethyl)-4-methyl-phenolato,L^{11}=Bis-1,5-((2-pyridylmethyl)amino)ethyl-3-thiapentane, L^{12} = diethanolamine, L^{13} = *N,N* -(ethane-1,2-diyldi-o-phenylene)-bis(pyridine-2-carboxamidide), L^{14} = triethanolamine, L^{15} = 2-pyridilpropanol and bba = 2-benzoylbenzoic acid, L^{16} = 2-formyl-4-methyl-6 *N*-ethylmorpholine -iminomethyl-phenolato, L^{17}=2-formyl-4-methyl-6 *N*-propylmorpholine-iminomethyl-phenolato, L^{18} = 2-(2-

pyridyl) benzimidazole, L^{19}= 4-amino antipyrine 1-naphthaldehyde, L^{20} = propylene sulfide and di-(2-pyridylmethyl) amine, L^{21} =1,3-bis(20-pyridylimino)isoindoline,L^{22}=*N,N*-[bis-(2-hydroxy-3-formyl-5-methylbenzyl) (dimethyl)]-ethylenediamine.]

Table S8. Kinetic parameters for the oxidation of *o*-aminophenol catalyzed by **1-3**.

Complexes	V_{max} (M min^{-1})	Std. error	K_M (M)	Std. error	k_{cat} (h^{-1})
1	1.05x 10^{-4}	2.06 x 10^{-6}	48.92 x10^{-4}	2.20 x 10^{-5}	126.8
2	9.91 x 10^{-5}	2.25 x 10^{-6}	44.00 x10^{-4}	3.06 x 10^{-5}	118.9
3	9.56 x 10^{-5}	2.69 x 10^{-6}	38.12 x10^{-4}	4.25 x 10^{-5}	114.7